Heliyon 6 (2020) e05272

Contents lists available at ScienceDirect

Heliyon

journal homepage: www.cell.com/heliyon

Research article

# Prediction of grass biomass from satellite imagery in Somali regional state, eastern Ethiopia

Derege Tsegaye Meshesha [a,b,*], Muhyadin Mohammed Ahmed [b], Dahir Yosuf Abdi [b], Nigussie Haregeweyn [c]

[a] Geospatial Data and Technology Centre, College of Agriculture and Environmental Science, Bahir Dar University, P.O. Box 79, Bahir Dar, Ethiopia
[b] Institute of Pastoral and Agro-Pastoral Development Studies (IPADS), Jigjiga University, P.O. Box 1020, Jigjiga, Ethiopia
[c] International Platform for Dryland Research and Education, Tottori University, 1390 Hamasaka, Tottori 680-0001, Japan

ARTICLE INFO

*Keywords:*
Drought-prone
IPADS
NDVI
EVI
Biomass
Remote sensing
Jigjiga university
Rangeland
Applied ecology
Ecosystem change
Environmental analysis
Natural resource management
Sustainable development
Ecology
Agriculture

ABSTRACT

The drought-prone Ethiopian Somali region has a long history of pastoralism (livestock grazing), which is a major source of livelihoods. However, it suffers from poor rangeland management and a lack of research and information. The objectives of this study were to develop a method for forecasting forage biomass and to quantify production of and spatial variation in forage from satellite imagery. We downloaded Sentinel-2 images and processed spectral information in the blue, red, and near-infrared bands, and calculated the Normalized Difference Vegetation Index (NDVI) and Enhanced Vegetation Index (EVI). Combining ground sampling (on 55 plots) with remote sensing data, we developed a forage forecasting model for the area. Forage (biomass) was significantly correlated with both EVI ($R^2 = 0.87$; $P < 0.001$) and NDVI ($R^2 = 0.81$; $P < 0.001$). Both gave good predictions of forage biomass in the district. We estimated the annual biomass in each grassland pixel at the peak of the growing season. Models based on each index revealed close estimates: NDVI indicated an average of 0.76 t/ha and a total of 38 772 t/year; EVI indicated an average of 0.78 t/ha and a total of 39 792 t/year. The estimated rangeland biomass showed high spatial variability of 0.22–4.89 t/ha.year. For future rangeland management in the area, the proposed approach and models can be used to estimate available forage biomass from satellite imagery in the middle of the grass growing season (2 months after the rains start), before the grass matures and is harvested.

## 1. Introduction

In Ethiopia, livestock constitute an important economic sector, contributing about 40% to the agricultural economy and supporting the livelihoods of about 80% of the rural community (FAO 2017). In the highlands, where mixed cultivation is the dominant agricultural system, cattle provide milk, meat and draught power for 95% of grain production (Asresie et al., 2015). Pastoral production is dominant in the arid and semiarid parts of the country (eastern, western and southern lowlands), which are highly susceptible to drought owing to the high inter-annual variability in rainfall (Schucknecht et al., 2015; Meshesha et al., 2019).

Even though Ethiopia has the largest livestock population in Africa, the contribution of livestock to the national economy is still the lowest (Solomon et al., 2003; Asresie et al. 2016). The current annual production of most rangelands in Ethiopia is not precisely known, so it is difficult to determine the current stocking rates and carrying capacities. Therefore, the status of rangelands and the balance between animal numbers and grassland resources (forage performance) are poorly understood in most parts of the country (Meshesha et al., 2019).

Both ground-based and remote-sensing techniques are used to estimate rangeland production (Liu et al., 2019). Traditional methods such as cutting $1m^2$ area and weight (Tucker et al., 1983; Bat-Oyun et al., 2016; Meshesha et al., 2019) are used to estimate the above-ground biomass (AGB). Recent advances in remote sensing and Geographical Information System (GIS) provide convenient techniques for the estimation of biomass (animal forage) with more accuracy than older techniques (Foody et al., 2003; Kumar et al., 2015; Fajji et al., 2018). The techniques enable rapid assessment of vegetation biomass over large areas relatively quickly and at low cost, overcoming many challenges involved in quantifying forage production across the landscape (Jin et al., 2014; Schucknecht et al., 2015; Liu et al., 2019; Kumar et al., 2015). In recent decades, different remote-sensing-based approaches have been

* Corresponding author.
*E-mail address:* deremesh@yahoo.com (D.T. Meshesha).

https://doi.org/10.1016/j.heliyon.2020.e05272
Received 16 October 2019; Received in revised form 24 January 2020; Accepted 10 October 2020
2405-8440/© 2020 Published by Elsevier Ltd. This is an open access article under the CC BY-NC-ND license (http://creativecommons.org/licenses/by-nc-nd/4.0/).

developed using optical (Steininger 2000; Thenkabail et al., 2004; Zheng et al., 2004), radar (Beaudoin et al., 1994; Sun et al., 2002; Solberg et al., 2010) and lidar (Patenaude et al., 2004; Hall et al., 2005; Saremi et al., 2014) data. However, owing to its broad coverage and cost-effectiveness, optical remote sensing is popular and provides a potential alternative to tedious hand-sampling as a means of estimating biomass over large areas (Kumar et al., 2015). Most studies use low-to medium-resolution optical data and an empirical relationship between field biomass measurements and remote sensing indicators popularly known as vegetation indices (VIs) (Eisfelder et al., 2011; Kumar et al., 2015).

The Somali regional state, where this study was conducted, has a long history of pastoralism (livestock grazing), which is a major source of livelihoods. Most of the Somali communities are pastoralists. Since 2000, informal protection of communal grazing lands (area enclosure) in the region, especially in Harshin district, has found favour (Meshesha et al., 2019).

However, despite the dominance of livestock production, the region suffers from poor rangeland management and limitation of research and information, mainly because of severe problems of peace and political instability in the past. Most recently, Meshesha et al. (2019) analysed the AGB productivity of rangelands, carrying capacity (CC), stocking rates and sustainability of grazing lands in Harshin district. In line with this, ABG includes all biomass of the grass and herbaceous above the soil including stems and foliage (Abbas et al., 2012) while carrying capacity refers to the maximum number of animals that the rangeland can support without depleting the resources of the rangeland (De Leeuw et al., 1990), and stocking rate is the number of animals on a grazing land for a specified time period (Cheng et al., 2017).

In the previous study, Meshesha et al. (2019) found a great disparity between stocking rate and carrying capacity, which if allowed to continue will lead to overgrazing and expansion of land degradation. However, the study did not address the spatial variation of biomass productivity.

The preparation of biomass production maps would help to boost the efficiency and sustainability of rangeland management by guiding pastoralists, resource managers and land use planners in the sustainable management of local grazing land. On the other hand, as to our knowledge, this kind of study using the methodology that we followed is carried out for the first time in Ethiopia and rarely in Africa. Hence, the study gives new knowledge and insight to international readers about this part of the world that can represent arid and semiarid regions of the world. Furthermore, the developed spectral model, which is properly calibrated and validated, can be applied to other part of the world which has similar agro-ecologies and climate such as Sahel and Sahara regions of Africa, and south east Asia.

Therefore, this study was designed with the purpose of developing a spatial model to support the forecasting of forage biomass and rangeland management in the Somali regional state with the aim of improving the accuracy and spatial limitations of existing systems. The specific objectives were (1) to develop a method of forecasting biomass from Sentinel-2 remote sensing data; (2) to validate the model in Harshin district; and (3) to scale up the model and quantify the production of and spatial variation in animal forage in the district.

## 2. Materials and methods

### 2.1. Study area

This study was carried out in Harshin district, within the Faafan zone of the Somali regional state of Ethiopia. It is located between $8^0$30′– 9°32′ N and 43°22’ – 44°18′ E (Figure 1). The district covers a total area of 5120 km$^2$ (BOFED 2012).

It has a moisture deficit due to limited rainfall (200–400 mm/y) and high temperatures (annual daily mean of 28 °C). The dominant soil types in the district are red-sandy soils, which has higher tendency of water porosity (less moisture retention). This limits the crop production potential of the district due to shortened moisture life to support plant growth and lower fertility status of the soil. There are 14 administrative units (kebeles) in the district. The latest census conducted in 2011 indicates that the population of Harshin district is about 92,901 people

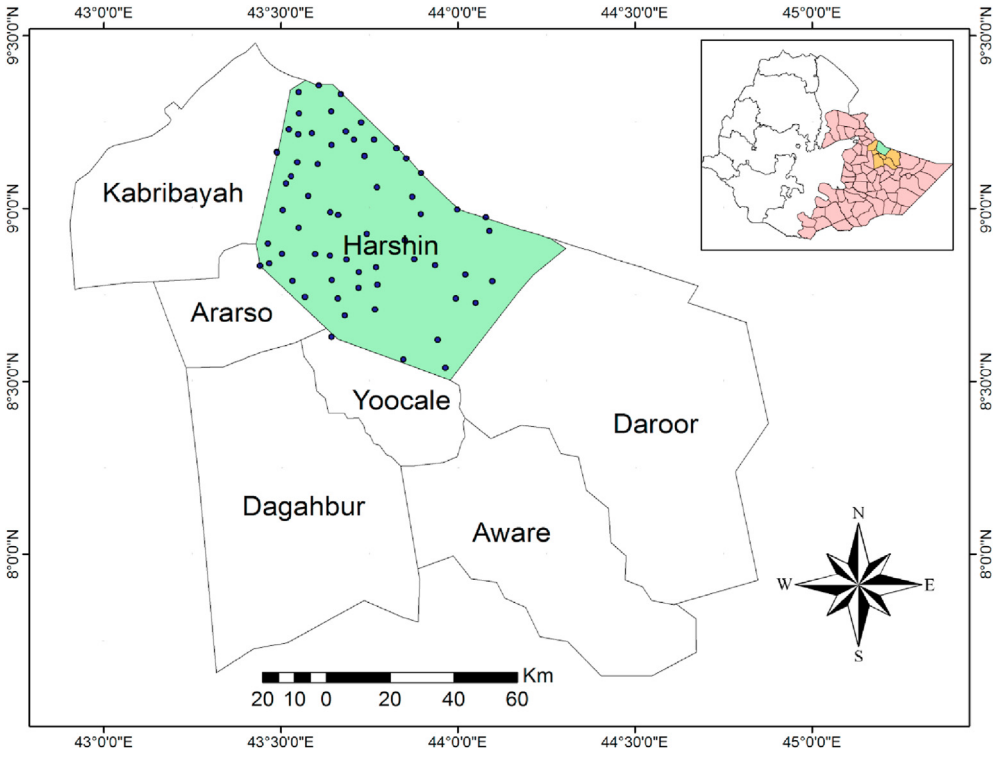


**Figure 1.** Location map of the study area: Harshin and its neighboring districts in Faafen zone, Eastern Somali regional state.

(90% rural and 10% urban) of whom 51,096 are men and 41,805 are women. The inhabitants of the district are entirely ethnic Somalis. Pastoralism is the dominant form of survival in the district, providing livelihood to over 70% of the population (BOFED 2012). The pastoralists rear many types of livestock, including dromedaries, cattle, sheep and goats. The predominant grazing pattern is based on seasonal movement between wet- and dry-season pastures (transhumance). Before 2000, the grazing areas were entirely communally owned. Since then, an informal protection of communal grazing lands (area enclosure) has been practised. This system brings good results in stocking grass for the dry season and has been widely adopted throughout the district.

### 2.2. Types of data and methods of collection

#### 2.2.1. Grass biomass data

First, we conducted a preliminary field survey (15–20 May 2018) before the start of the rainy season, and selected plots in which to measure AGB of grass. We selected 55 plots at two sites and geo-marked them by GPS for further investigation, monitoring and productivity measurement. To be selected, a plot had to cover at least 0.5 ha so that it could conform to the pixel size of most of the freely available satellite images without being affected by reflection from nearby features or land cover. At both sites, humans and animals were excluded until we had measured biomass. The sites were selected as being representative of the district: site 1 represented high forage production, and site 2 represented medium to low production. We measured AGB in summer (while grass is maturing) in 13 high-, 17 medium- and 25 low-production plots.

The best time to measure the grass biomass is mid-July, when the grass has matured and dried. We threw a 1-$m^2$ quadrat into each plot and cut the forage in it at ground level with shears. We weighed the fresh sample on a balance and used a moisture correction factor (Gay et al., 2009) to calculate the total dry matter (TDM) (Meshesha et al., 2019). The TDM was converted to kg/ha and multiplied by 30% to calculate the content available for animal consumption (Meshesha et al., 2019).

#### 2.2.2. Remote sensing dataset and processing

We downloaded cloud-free satellite images (acquired on 11 May 2018 by Sentinel-2 sensors) and prepared a land use and cover map of the district.Sentinel-2 data are acquired in 13 spectral bands in the visible and near-infrared (NIR) region and the short-wave infrared (SWIR) region at a spatial resolution that depends on the band. We used four bands (B2, B3, B4, B8) with a 10-m resolution for feature identification. Then we carried out hybrid unsupervised and supervised classification to identify and extract grasslands. In line with this, grass biomass and crop yield model development and forecasting are often dependent on 3 seasons or plant phenology: seedling, flowering and maturity (Burke and David, 2016; Monteith, 1972). Thus, in our case, we deliberately selected the acquisition time (May 11) to be the flowering stage (about 2 month since the rain starts) taking into consideration high canopy cover at this time and to minimize the influence from soil reflectance.

We also used Garmin GPSMAP 64 navigators with a reported 3-m accuracy to collect representative ground truth data for each form of land use and cover in the district, at a total of 170 ground control points. The image classification accuracy of each land use and cover was analysed using the ground truth data. Thereby, an overall accuracy of greater than 88% was computed which is sufficient to proceed with next analysis (Table 1).

### 2.3. Development of vegetation indices (VI) and biomass estimation models

A vegetation index (also called a vegetative index) is a single number that quantifies vegetation biomass and/or plant vigour using a spectral transformation of two or more bands (Huete et al., 2002). In the use of remote sensing to estimate above-ground biomass, the spectral reflectance value is highly affected by plant health and canopy parameters such as leaf area index, chlorophyll content, maturity and plant density (Kumar et al., 2015). Thus, plants in better health, with greater leaf area index, and at greater plant density will have higher reflectance in some bands (e.g., NIR and SWIR) than plants of the same species but under some kind of stress, such as disease, low soil moisture or poor soil fertility.

One of the most widely used VI is the Normalized Difference Vegetation Index (NDVI; Gaitán et al., 2013; Ouyang et al., 2012). NDVI values range from −1.0 to +1.0. Areas of barren rock, sand, or snow usually have very low NDVI values (for example, ≤0.1). Sparse vegetation such as shrubs and grassland has moderate NDVI values (~0.2–0.5). Dense vegetation such as that found in temperate and tropical forests or in crops at their peak growth stage has high NDVI values (0.6–0.9). NDVI can be downloaded directly from Landsat and other data sets and used directly to estimate biomass (https://www.usgs.gov/archive-normalized-difference-vegetation-index-ndvi-composites). Another is the Enhanced Vegetation Index (EVI), which sometimes offers better performance (Jin et al., 2014; Kumar et al., 2015; Meshesha et al., 2018). However, unlike NDVI, it is not directly available in different datasets rather needs calculation using the necessary bands.

We processed the Sentinel-2 images in the blue (0.44–0.53 μm), green (0.54–0.58 μm), red (0.65–0.69 μm) and NIR (0.78–0.91 μm) bands. Blue and red are important for photosynthesis, so healthy vegetation always has low reflection in these bands (Monteith et al. 1972; Burke and David 2016). The NIR band has the highest reflectance from vegetation (Slaton et al., 2001). We calculated NDVI and EVI in ArcGIS v. 10.2.2 software as:

$$NDVI = (NIR - Red) / (NIR + Red) \quad \text{(Eq. 1)}$$

$$EVI = 2.5 \times (NIR - red) / (NIR + [6 \times red] + [7 \times blue] + 1) \quad \text{(Eq. 2)}$$

We calculated the VI values of grasses at the selected plots and established a database of VI versus biomass values. Then we built regression models that relate the NDVI and EVI values to the field-measured biomass. We then evaluated the models and used them to quantify the spatial variance of forage biomass in the district. In statistical modeling, regression analysis is an arithmetic procedure for

**Table 1.** Summary of land-use/cover image classification accuracy (2018).

| Ground truth | Classified data (2018) | | | | | | |
|---|---|---|---|---|---|---|---|
| | Grassland | Shrubland | Bareland | Woodland | Total | Producer[a] (%) | User[b] (%) |
| Grassland | 53 | 0 | 3 | 0 | 56 | 95% | 91% |
| Shrubland | 0 | 32 | 0 | 6 | 38 | 84% | 89% |
| Bareland | 5 | 0 | 35 | 0 | 40 | 88% | 92% |
| Woodland | 0 | 4 | 0 | 32 | 36 | 89% | 84% |
| Total | 58 | 36 | 38 | 38 | 170 | | |
| Overall accuracy | 89% | | | | | | |

[a] Producer indicates the proportion that the given land-use/cover class is not classified as other class.
[b] User indicates the proportion that other classes are not categorized as a given land use/cover.

determining the association between the dependent variable (often called the outcome, and in our case the "grass biomass value") and the independent variables (often called predictors, and in our case the "vegetation index value"). Thus, the regression analysis is primarily used to understand the relationships between the independent and dependent variables and widely used for prediction and forecasting of one variable from the other (Freedman, 2009). The most common form of regression analysis is linear regression. However, in our study, we tested different type of functions (e.g. linear, exponential, power-law, logarisim and polynomial function) and the most fitted curved between the indices and biomass has become polynomial function.

### 2.4. Calibration and validation of models

We divided the observed data into odd and even plot numbers, and used odd numbers (28 plots) for model calibration (by regression equation) and even numbers (27 plots) for validation. To evaluate model performance, we compared predicted and measured biomass values and determined $R^2$. To evaluate the model accuracy, we calculated the root-mean-square error (RMSE) and the mean relative estimation error (REE) from the validation data. Finally, we selected the best model according to $R^2$ and the precision. All statistical analyses were performed in Excel (2010) software. *ME* and *RRMSE* were calculated as:

$$ME = 1 - \frac{\sum_{i=1}^{n}(O_i - P_i)^2}{\sum_{i=1}^{n}(O_i - O_{mean})^2} \quad (3)$$

$$RRMSE = \frac{\sqrt{\frac{1}{n}\sum_{i=1}^{n}(O_i - P_i)^2}}{\frac{1}{n}\sum_{i=1}^{n} O_i} \quad (4)$$

where $n$ is the number of observations, $O_i$ is the observed value, $P_i$ is the predicted value, and $O_{\text{mean}}$ is the mean observed value.

## 3. Results and discussion

### 3.1. Forage biomass prediction models

The NDVI and EVI maps are shown in Figures 2 and 3, respectively. The extracted NDVI and EVI values of the ground control points were significantly correlated with the measured forage biomass data: NDVI with $R^2 = 0.81$ ($P < 0.001$; Eq. 5) and EVI with $R^2 = 0.87$ ($P < 0.001$; Eq. 6).

Both gave good predictions of forage biomass (at 2 months after rains start and 2 months before maturity) in Harshin district.

$$\text{Forage biomass (t/ha.year)} = 11.59(\text{NDVI})^2 – 4.96(\text{NDVI}) + 0.76 \quad \text{(Eq. 5)}$$

$$\text{Forage biomass (t/ha.year)} = 11.21(\text{EVI})^2 + 0.27(\text{EVI}) + 0.038 \quad \text{(Eq. 6)}$$

The results imply that although NDVI is widely used and gives good results, it may not always be the best VI in all regions and on all vegetation types (as seen in our study area). Gill et al. (2009) found that NDVI had limitations in biomass estimation since values becomes saturated at higher levels of biomass (dense vegetation), and thus they suggested the use of other VIs such as EVI, which can overcome the saturation problem. Mutanga and Skidmore (2004) reported that the NDVI performed poorly in estimating the biomass of savannah in Kruger National Park in South Africa, explaining that it showed a non-linear response and was less sensitive to differences at very low and very high vegetation densities. Other studies have also revealed limitations or the sensitivity of NDVI to herbaceous biomass of savannahs in the Sahel zone of Senegal (Tucker et al., 1985; Diallo et al., 2007). Similar studies conducted in the desert steppe region of China (similar to our grassland plains and shrubs), the values of $R^2$ of biomass versus EVI, soil-adjusted VI and modified soil-adjusted VI were higher than that of biomass versus NDVI (Jin et al., 2014).

This variation in results implies that correlations between VI and biomass, as well as the efficiencies of VI models at predicting biomass, vary from place to place depending on species, density and spatial heterogeneity of biomass among grassland types. Thus, as suggested by Jin

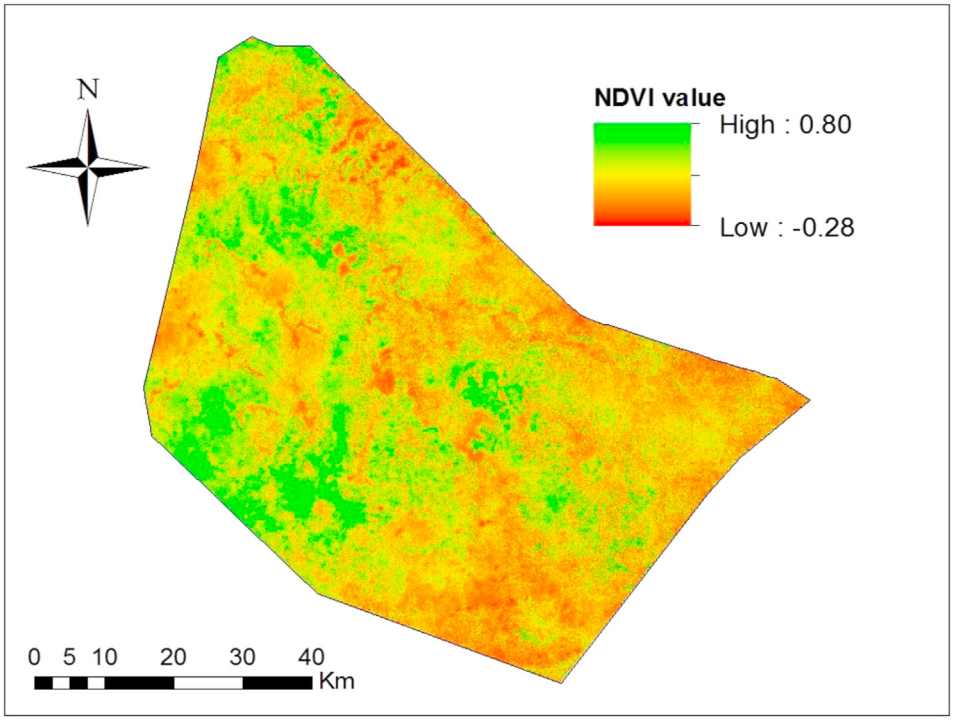


**Figure 2.** NDVI calculated map of Harshin district.

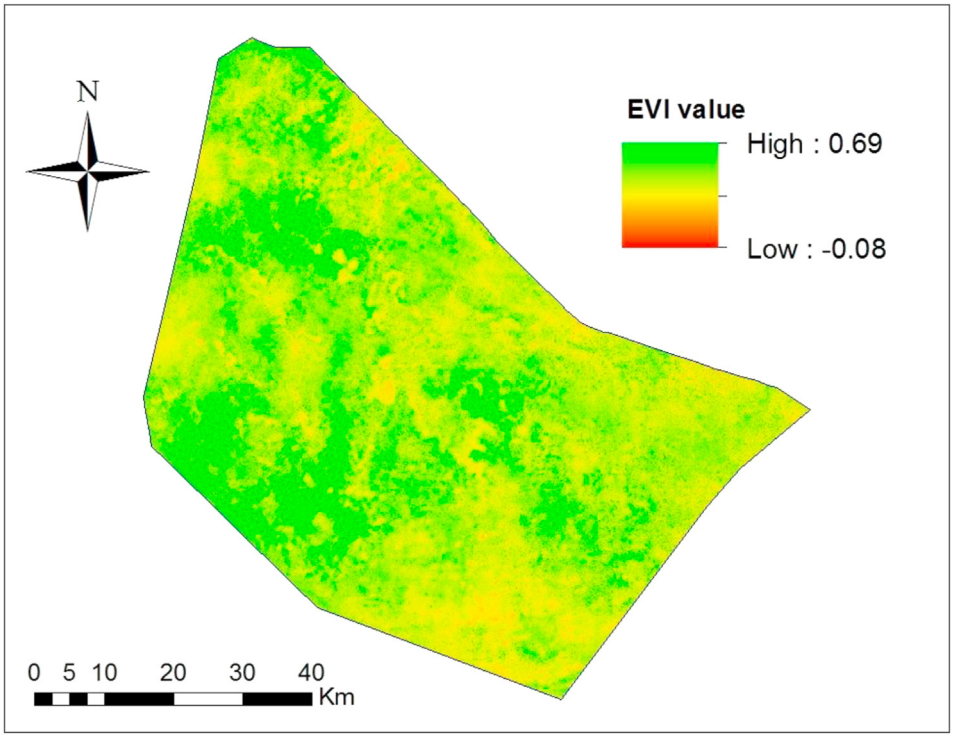


**Figure 3.** EVI calculated map of Harshin district.

et al. (2014), biomass estimates should depend on the most appropriate remote sensing estimation model developed for a particular area and grassland type, rather than on a model developed in a different region.

### 3.2. Model calibration and validation

Among the models, polynomial function models relating NDVI and EVI to biomass showed the best performance. EVI had slightly better fitness and correlation with forage biomass (Figure 4). In validation, the EVI model explained about 92% of the forage biomass variability in the district and had an error of 0.21, and the NDVI model explained about 87% and had an error of 0.26 (Figure 5). Thus, the results of both models are acceptable for wide-scale prediction of biomass in the district, and could be further calibrated and validated to apply to other districts and zones in the region.

### 3.3. Quantifying and mapping the spatial distribution of forage biomass

From the land use and cover map of the district (Figures 6-1), we selected grassland pixels (Figure 6-2) at which to calculate NDVI and EVI values.

The polynomial function regression models then transformed the spatial index maps to forage biomass maps, which showed the estimated annual grassland biomass in each pixel at the peak period of the growing season (about 2 months after the rains start). Thereby, the NDVI and EVI based grass biomass estimations are presented below (Figures 7 and 8).

The models estimates agreed closely in all biomass parameters (minimum, maximum, average and SD; Figure 9). The NDVI model gave an average of 0.76 t/ha.year and a total of 38 772 t/y; the EVI model gave an average of 0.78 t/ha and a total of 39 792 t/year. Future rangeland management will benefit from the advance prediction of available

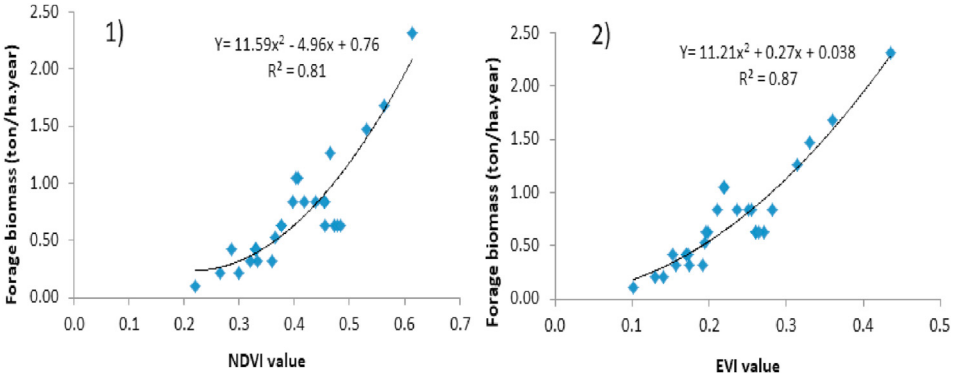


**Figure 4.** Results of model calibration for NDVI (1) and EVI (2).

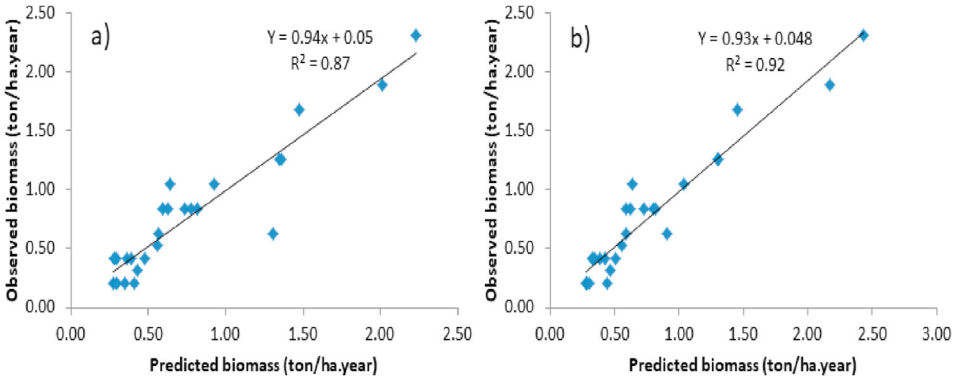


**Figure 5.** Results of model validation for NDVI (a) and EVI (b) indexes.

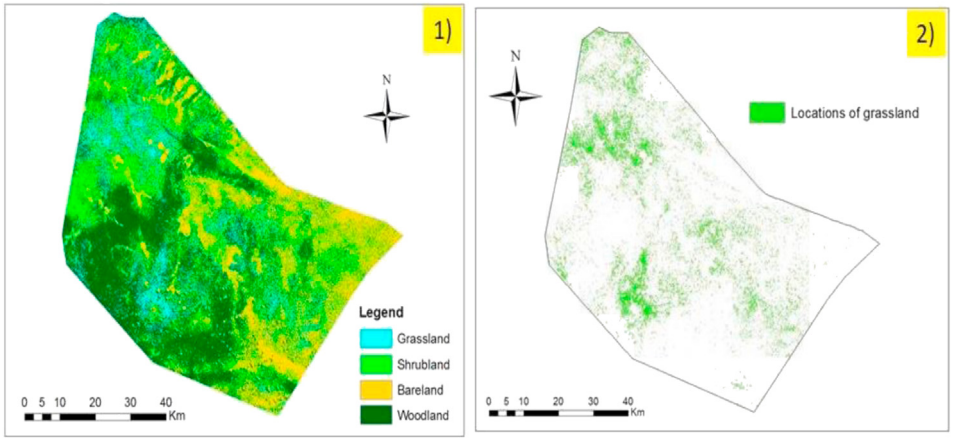


**Figure 6.** Land use and cover map of Harshin (1) as dervied from Sentinel 2 (June 2018); Spatial distribution of grassland pixel in the district (2).

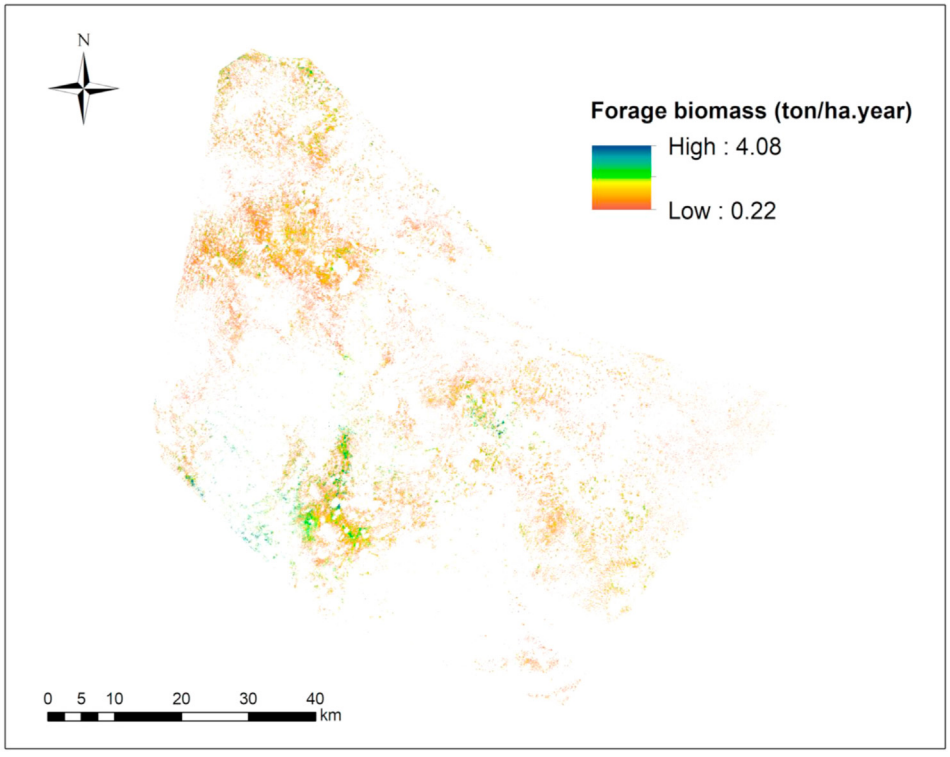


**Figure 7.** Estimation of forage biomass using transformed NDVI index.

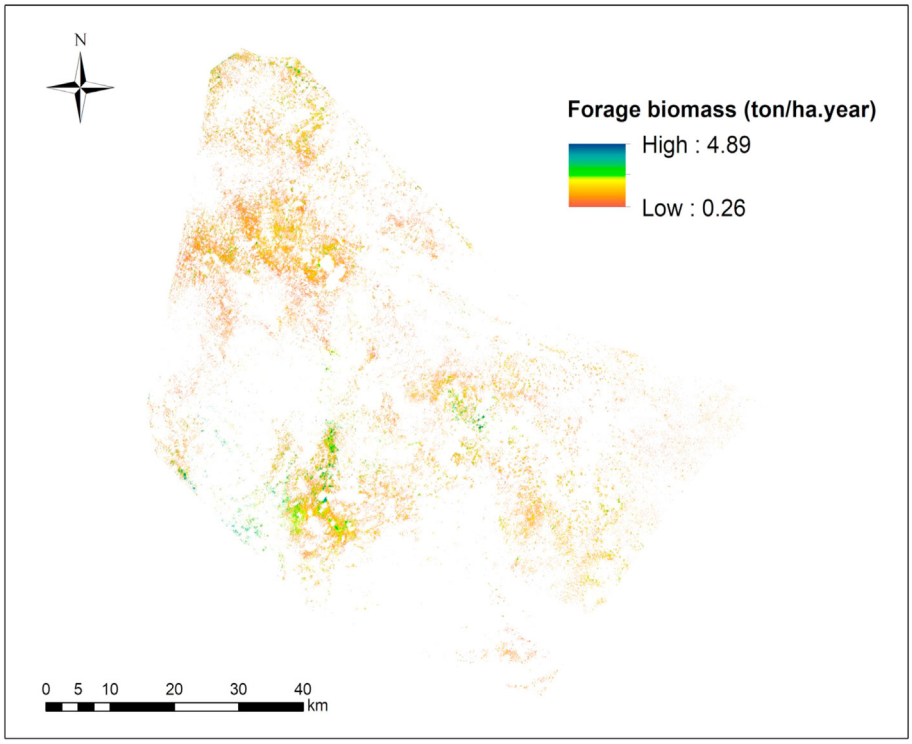


**Figure 8.** Estimation of forage biomass using transformed EVI index.

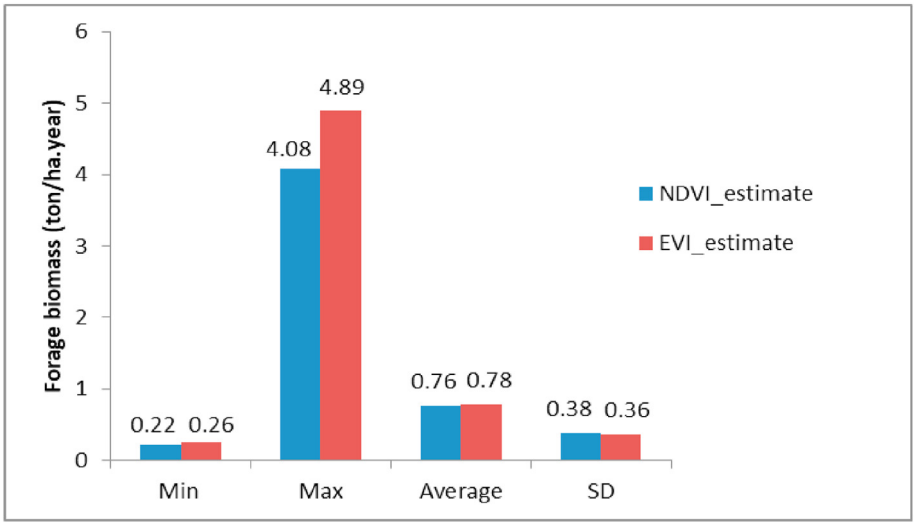


**Figure 9.** Summary of forage biomass estimation values for Harshin (as derived from NDVI and EVI transformed maps).

biomass from satellite imagery just 2 months after the rains start and 2 months before maturity.

The remote-sensing-based estimates of biomass in Harshin district are comparable to a ground-measured value of 0.74 t/ha and a total of 37 884 t/y (Meshesha et al., 2019). Our results are more or less in line with those of Schucknecht et al. (2015) in Niger (0.35–1.78 t/ha, average 0.74 t/ha), of Jin et al. (2014) in China (0.4–0.85, average 0.62) and of Ramoelo et al. (2012) in South Africa (0.22–1.53 t/ha, average 0.8 t/ha). The average values in all of these comparisons are close, although the maximum values vary a bit, perhaps being limited to a few pixels that do not represent the majority. Our results are comparable to values measured on the ground by Rains and Kassam (1979) in West Africa (0.5–1.7 t/ha), but lower than those measured by van Wijngaarden (1985) in eastern Kenya (2.3 t/ha) and by Dye and Spear (1982) in Zimbabwe (1.7 t/ha). These comparisons imply that forage production in Harshin district is moderate.

### 3.4. Spatial variation in forage biomass in Harshin district

The biomass estimates ranged widely between 0.22 and 4.89 t/ha.year (Figure 9). Most of the grasslands are located in the north-western and south-western parts of the district (Figure 6). However,

most of the pixels with the highest production are located in the south-western part, where growth conditions and grassland resources are better (Figures 7 and 8). Most of the pixels in the north had the lowest productivity (<2 t/ha/y), which indicates that they have very low potential to support cattle, owing to the presence of large areas of bare soil (Figure 6). Nevertheless, such sites have good potential for browsers (e.g. goats) owing to the presence of browsable shrubs such as short *Acacia*. The variation in biomass production in the study area might be explained by soil type, behaviours of grazers, or landscape or other biophysical factors, as forage productivity, composition and spatial distribution in rangeland ecosystems are controlled mainly by climate, soil properties and behaviours of herbivores (Wiegand et al., 2006; Higgins et al., 2007). Furthermore, mean annual precipitation of rangelands and animal behaviours are major factors in the variation of grass biomass production (Wiegand et al., 2006; Scholes 2009).

### 3.5. Specifications and limitations: caution when applying the models

The models are based on spectral data (satellite imagery) taken at a specific stage of grass phenology (flowering period). In the district, rain started on 13 March 2018, imagery was acquired on 11 May (2 months later), and ground-truth measurement was carried out on 15–20 July 2018. Thus, the models are expected to estimate forage biomass about 2 months after the rains start and 2 months before forage maturity (harvest). The rains may start earlier or later than our date, but images to be used for prediction should be acquired about 2 months (plus or minus 2 weeks) after the rains start, because reflectance and index values might be higher or lower if images are downloaded much earlier or later. Thus, a range of ±2 weeks do not greatly change reflectances. However, if images are taken too early (e.g. one month after the rain starts), the reflectance from the grass will be heavily affected by the bare soil and hence the vegetation index values from the grass will be lower, and that will underestimate the biomass value during the prediction. On the other hand, if the images are taken too late (e.g. three months since the rain starts), the grass appears grey and will have lower index value, and similarly that will affect (underestimate) the precision during the prediction. Thus, this fact and preconditions should be taken into consideration when the model is applied to predict grass biomass in any part of the world.

## 4. Conclusions

The aims of this research were to develop a model to estimate forage biomass from remote sensing data, and to assess the current production of and spatial variation in forage biomass in Harshin district.

Model calibration revealed that forage biomass was better correlated with EVI ($R^2 = 0.87$; $P < 0.001$) than NDVI ($R^2 = 0.81$; $P < 0.001$). Polynomial functions based on both VIs gave the most accurate predictions: the EVI-based model explained about 92% of the forage biomass variability in the district, and the NDVI-based model explained about 87%.

The NDVI-based model estimated the average biomass of the area to be 0.76 t/ha and the total to be 38 772 t/y. The EVI-based model estimated 0.78 t/ha and 39 792 t/y. The ground-measured biomass had high spatial variability, ranging from 0.22 to 4.89 t/ha.year.

These models can be used to estimate total forage biomass available to feed livestock in 2 months before harvest, and that helps pastoralists and land managers to better manage the sustainability of grazing land. Furthermore, this pioneer research to the region might encourage other researchers to conduct similar researches in the area where such studies are rare.

## Declarations

### Author contribution statement

Derege Tsegaye Meshesha: Conceived and designed the experiments; Performed the experiments; Analyzed and interpreted the data; Contributed reagents, materials, analysis tools or data; Wrote the paper.

Muhyadin Mohammed Ahmed: Conceived and designed the experiments; Performed the experiments; Analyzed and interpreted the data; Contributed reagents, materials, analysis tools or data.

Dahir Yosuf Abdi, Nigussie Haregeweyn: Performed the experiments; Contributed reagents, materials, analysis tools or data.

### Funding statement

This research did not receive any specific grant from funding agencies in the public, commercial, or not-for-profit sectors.

### Competing interest statement

The authors declare no conflict of interest.

### Additional information

No additional information is available for this paper.

## References

Abbas, S., Saleem, A., Sharif, Z., Mirza, S., 2012. Estimation of biomass and carrying capacity of scrub rangelands in ucchali wetland complex, soon valley. Biologia 58 (1&2), 93–100.

Asresie, A., Zemedu, L., 2015. Contribution of livestock sector in Ethiopian economy: a review. Adv. Life Sci. Technol. 29, 79–90.

Bat-Oyun, S., Shinoda, M., Cheng, Y., Purevdorj, Y., 2016. Effects of grazing and precipitation variability on vegetation dynamics in a Mongolian dry steppe. J. Plant Ecol. 9, 508–519.

Beaudoin, A., Le Toan, T., et al., 1994. Retrieval of forest biomass from SAR data. Int. J. Rem. Sens. 15, 2777–2796.

BOFED (Bureau of Finance and Economic Development), 2012. Somali Region, Jijiga, Ethiopia.

Burke, M., David, L.B., 2016. Satellite-based Assessment of Yield Variation and its Determinants in Smallholder African Systems. Department of Earth System Science, Stanford University, CA, USA.

Cheng, D., Peili, S., Xianzhou, Z., Ning, Z., Xi, C., Wanrui, Z., 2017. The rangeland livestock carrying capacity and stocking rate in the Kailash sacred landscape in China. J. Resour. Ecol. 8 (6), 551–558.

De Leeuw, P.N., Tothill, J.C., 1990. The Concept of Rangeland Carrying Capacity in Sub-saharan Africa: Myth or Reality? ODI. Pastoral Development Network Paper 29b, London Uk, p. 20.

Diallo, O., Diouf, A., Hanan, N.P., Ndiaye, A., Prevost, Y., 2007. AVHRR monitoring of savanna primary production in Senegal, West Africa: 1987–1988. Int. J. Rem. Sens. 12 (6), 1259–1279.

Dye, P.J., Spear, P.T., 1982. The effects of bush clearing and rainfall variability on grass yield and composition in southwest Zimbabwe. Zimbabwe J. Agric. Res. 20, 103–118.

Eisfelder, C., Kuenzer, C., Dech, S., 2011. Derivation of biomass information for semi-arid areas using remote-sensing data. Int. J. Rem. Sens. 33 (9), 2937–2984.

Fajji, N.G., Palamuleni, L.G., Mlambo, V., 2018. A GIS scheme for forage assessment and determination of rangeland carrying capacity. J. Remote Sens. GIS.

FAO, 2017. Africa Sustainable Livestock 2050 – Technical Meeting and Regional Launch, Addis Ababa, Ethiopia, 21–23 February 2017. FAO Animal Production and Health Report. No. 12. Rome, Italy.

Foody, G.M., Boyd, D.S., Cutler, M.E.J., 2003. Predictive relations of tropical forest biomass from Landsat TM data and their transferability between regions. Rem. Sens. Environ. 85, 463–474.

Freedman, D.A., 2009. Statistical Models: Theory and Practice. Cambridge University Press.

Gaitán, J.J., Bran, D., Oliva, G., Ciari, G., Nakamatsu, V., Salomone, J., Ferrante, D., Buono, G., Massara, V., Humano, G., 2013. Evaluating the performance of multiple remote sensing indices to predict the spatial variability of ecosystem structure and functioning in Patagonian steppes. Ecol. Indicat. 34, 181–191.

Gay, S.W., Grisso, R., Smith, E., 2009. Determining Forage Moisture Concentration. Produced by Communications and Marketing, College of Agriculture and Life Sciences. Virginia Polytechnic Institute and State University.

Gill, T.K., Phinn, S.R., Armstong, J.D., Pailthorpe, B.A., 2009. Estimating tree-cover change in Australia: challenges of using the MODIS vegetation index product. Int. J. Rem. Sens. 30 (6), 1547–1565.
Hall, S.A., Burke, I.C., Box, Do., Kaufmann, M.R., Stoker, J.M., 2005. Estimating stand structure using discrete-return lidar: an example from low density, fire prone ponderosa pine forests. For. Ecol. Manag. 208 (1–3), 189–209.
Higgins, S.I., Bond, W.J., February, E.C., Bronn, A., Euston-Brown, D.I.W., et al., 2007. Effects of four decades of fire manipulation on woody vegetation structure in savanna. Ecology 88, 1119–1125.
Huete, A., Didan, K., Miura, T., Rodriguez, E.P., Gao, X., Ferreira, L.G., 2002. Overview of the radiometric and biophysical performance of the MODIS vegetation indices. Remote Sens. Environ. 83, 195–213.
Jin, Y., Yang, X., Qiu, J., Li, J., Gao, T., Wu, Q., Zhao, F., Ma, H., Yu, H., Xu, B., 2014. Remote sensing-based biomass estimation and its spatio-temporal variations in temperate grassland, Northern China. Rem. Sens. 6, 1496–1513.
Kumar, L., Sinha, P., Taylor, S., Alqurashi, A.F., 2015. Review of the use of remote sensing for biomass estimation to support renewable energy generation. J. Appl. Remote Sens. 9, 097696.
Liu, H., Dahlgren, R.A., Larsen, R.E., Devine, S.M., Roche, L.M., et al., 2019. Estimating rangeland forage production using remote sensing data from a small unmanned aerial system (sUAS) and PlanetScope satellite. Rem. Sens.
Meshesha, D.T., Abeje, M., 2018. Developing crop yield forecasting models for four major Ethiopian agricultural commodities. Remote Sens. Appl.: Soc. Environ. 11, 83–93.
Meshesha, D.T., Mohammed, M., Yosuf, D., 2019. Estimating carrying capacity and stocking rates of rangelands in Harshin District, eastern Somali Region, Ethiopia. Evol. Ecol.
Monteith, J.L., 1972. Solar radiation and productivity in tropical ecosystems. J. Appl. Ecol. 9, 747–766.
Mutanga, O., Skidmore, A.K., 2004. Hyperspectral band depth analysis for a better estimation of grass biomass (*Cenchrus ciliaris*) measured under controlled laboratory conditions. Int. J. Appl. Earth Obs. Geoinf. 5, 87–96.
Ouyang, W., Hao, F.H., Skidmore, A.K., Groen, T.A., Toxopeus, A.G., Wang, T.J., 2012. Integration of multi-sensor data to assess grassland dynamics in a Yellow River sub-watershed. Ecol. Indicat. 18, 163–170.
Patenaude, G., Hill, R.A., Milne, R., Rowland, C.S., Dawson, T.P., 2004. Quantifying forest aboveground carbon using LiDAR remote sensing. Remote Sens. Environ. 93 (3), 368–380.
Rains, A.B., Kassam, A.H., 1979. Land Resources and Animal Production Consultants' Working Paper No 8 FAO/UNFPA Project INT/75/P13 AGLS FAO, Rome, p. 28.
Ramoelo, A., Skidmore, A.K., Cho, M.A., Schlerf, M., Mathieu, R., Heitkőnig, I.M.A., 2012. Regional estimation of savannah grass nitrogen using red edge band of the RapidEye sensor. Int. J. Appl. Earth Obs. Geoinf. 19, 151–162.
Saremi, H., Kumar, L., Christine Stone, C., Melville, G., Turner, R., 2014. Sub-compartment variation in tree height, stem diameter and stocking in a Pinus radiata D. Don plantation examined using airborne LiDAR data. Rem. Sens. 6 (8), 7592–7609.
Scholes, R.J., 2009. Syndromes of dry-land degradation in southern Africa. Afr. J. Range Forage Sci. 26, 113–125.
Schucknecht, A., Meroni, M., Kayitakire, F., Rembold, F., Boureima, A., 2015. Biomass estimation to support pasture management in Niger. In: The International Archives of the Photogrammetry, Remote Sensing and Spatial Information Sciences, Volume XL-7/W3. The 36th International Symposium on Remote Sensing of Environment, 11–15 May 2015, Berlin, Germany.
Slaton, M.R., Hunt, E.R., Smith, W.K., 2001. Estimating near infrared leaf reflectance from leaf structural characteristics. Am. J. Bot. 88, 278–284.
Solberg, S., Astrup, R., Gobakken, T., Næsset, E., Weydahl, D.J., 2010. Estimating spruce and pine biomass with interferometric X-band SAR. Rem. Sens. Environ. 114 (10), 2353–2360.
Solomon, A., Workalemahu, A., Jabbar, M.A., Ahmed, M.M., Hurissa, B., 2003. Livestock Marketing in Ethiopia: a Review of Structure, Performance and Development Initiatives. ILRI Socio-Economic and Policy Research Working Paper 52.
Steininger, M.K., 2000. Satellite estimation of tropical secondary forest above-ground biomass: data from Brazil and Bolivia. Int. J. Rem. Sens. 21 (6–7), 1139–1157.
Sun, G., Ranson, K.J., Kharuk, V.I., 2002. Radiometric slope correction for forest biomass estimation from SAR data in the Western Sayani Mountains, Siberia. Remote Sens. Environ. 79 (2–3), 279–287.
Thenkabail, P.S., Stucky, N., Griscom, B.W., Ashton, M.S., Diels, J., van der Meer, B., Enclona, E., 2004. Biomass estimations and carbon stock calculations in the oil palm plantations of African derived savannas using IKONOS data. Int. J. Rem. Sens. 25 (23), 5447–5472.
Tucker, C.J., van Praet, C., Boerwinkle, E., Gaston, A., 1983. Satellite remote sensing of total dry matter accumulation in the Senegalese Sahel. Rem. Sens. Environ. 13, 461–474.
Tucker, C.J., Vanpraet, C.L., Sharman, M.J., Van Ittersum, G., 1985. Satellite remote sensing of total herbaceous biomass production in the Senegalese Sahel: 1980–1984. Remote Sens. Environ. 17 (3), 233–249.
van Wijngaarden, W., 1985. Elephants-Trees-Grass-Grazers: Relationships between Climate, Soils, Vegetation and Large Herbivores in a Semi-arid Ecosystem (Tsavo, Kenya). ITC Publ No 4 Enschede, Netherlands.
Wiegand, K., Saltz, D., Ward, D., 2006. A patch dynamics approach to savanna dynamics and woody plant encroachment – insights from an arid savanna. Perspect. Plant Ecol. Evol. Systemat. 7, 229–242.
Zheng, D., Rademacher, J.M., Chen, J., Crow, T.R., Bresee, M.K., Moine, J.M., Ryu, S.R., 2004. Estimating Aboveground Biomass Using Landsat 7 ETM+ Data across a Managed Landscape in Northern Wisconsin, USA.